Structural Characterization of a Human-Type Corrinoid Adenosyltransferase Confirms That Coenzyme B_{12} Is Synthesized through a Four-Coordinate Intermediate[†,‡]

Martin St. Maurice,[▽] Paola Mera,[§] Kiyoung Park,[||] Thomas C. Brunold,[||] Jorge C. Escalante-Semerena,[§] and Ivan Rayment*,[▽]

Departments of Biochemistry, Bacteriology, and Chemistry, University of Wisconsin, Madison, Wisconsin 53706

Received January 23, 2008; Revised Manuscript Received March 12, 2008

ABSTRACT: ATP:cob(I)alamin adenosyltransferases (ACAs) catalyze the transfer of the 5′-deoxyadenosyl moiety from ATP to the upper axial ligand position of cobalamin in the synthesis of coenzyme B_{12}. For the ACA-catalyzed reaction to proceed, cob(II)alamin must be reduced to cob(I)alamin in the enzyme active site. This reduction is facilitated through the generation of a four-coordinate cob(II)alamin intermediate on the enzyme. We have determined the high-resolution crystal structure of a human-type ACA from *Lactobacillus reuteri* with a four-coordinate cob(II)alamin bound in the enzyme active site and with the product, adenosylcobalamin, partially occupied in the active site. The assembled structures represent snapshots of the steps in the ACA-catalyzed formation of the cobalt−carbon bond of coenzyme B_{12}. The structures define the corrinoid binding site and provide visual evidence for a base-off, four-coordinate cob(II)alamin intermediate. The complete structural description of ACA-mediated catalysis reveals the molecular features of four-coordinate cob(II)alamin stabilization and provides additional insights into the molecular basis for dysfunction in human patients suffering from methylmalonic aciduria.

Coenzyme B_{12} [adenosylcobalamin (AdoCbl)][1] is an organometallic cofactor required in a variety of metabolic reactions (*1*). In mammals, AdoCbl is used exclusively by the enzyme methylmalonyl-CoA mutase, which participates in the catabolism of various amino acids, odd chain fatty acids, and cholesterol (*2, 3*). Humans are unable to synthesize AdoCbl de novo. Consequently, cobalamin [vitamin B_{12} (CNCbl)] (Figure 1A) must be ingested, absorbed, and transported to the mitochondria, where an ATP:cob(I)alamin adenosyltransferase (ACA) catalyzes the transfer of the 5′-deoxyadenosyl moiety of ATP to the upper axial ligand position of cobalamin (Cbl), generating AdoCbl (Figure 1). Patients with malfunctions in ACA are impaired in their ability to generate this cofactor and suffer from methylmalonic aciduria, a rare but potentially fatal disease characterized by an accumulation of methylmalonic acid in the blood and urine (*4*).

The reaction catalyzed by ACA enzymes proceeds through a direct, nucleophilic attack from the Co^{+} of cob(I)alamin to the 5′-carbon of ATP (Figure 1C). When ingested as vitamin B_{12}, Cbl is in the Co^{3+} oxidation state. Thus, two one-electron reductions of the corrin cobalt [cob(III)alamin → cob(II)alamin → cob(I)alamin] are required to generate the reactive Co^{+} nucleophile. The standard potential for reduction of aquacob(III)alamin to cob(II)alamin is 200 mV versus the standard hydrogen electrode (SHE) (*5*), and this reduction occurs easily within the reducing intracellular environment (*6*). However, the subsequent reduction of cob(II)alamin to cob(I)alamin has a reduction potential of −610 mV versus the SHE (*5*), significantly lower than the reduction potential of available in vivo reducing agents (*7, 8*). Spectroscopic evidence supports the idea that ACA enzymes bind cob(II)alamin and convert it to a rare, base-off, four-coordinate intermediate exclusively in the presence of the ATP substrate (*8–10*). This conversion raises the redox potential of the cob(II)alamin/cob(I)alamin couple and facilitates the final electron transfer from an electron transfer protein or an associated reductase (*11–13*). The resulting cob(I)-alamin "supernucleophile" is poised to attack the 5′-carbon

[†] This work was supported in part by Public Health Service Grants AR35186 (to I.R.) and R01-GM40313 (to J.C.E.-S.) from the National Institutes of Health and Grant MCB-0238530 (to T.C.B.) from the National Science Foundation. P.M. was supported in part by Chemical Biology Interface Training Grant T32-GM008505 (L. L. Kiessling, Principal Investigator) from the National Institute of General Medical Sciences.

* To whom correspondence should be addressed: Department of Biochemistry, University of Wisconsin, 433 Babcock Dr., Madison, WI 53706. E-mail: Ivan_Rayment@biochem.wisc.edu. Phone: (608) 262-0437. Fax: (608) 262-1319.

[‡] The atomic coordinates and structure factors for the complexes of LrPduO with ATP:cob(II) alamin, tripolyphosphate:adenosylcobalamin, and ATP:cob(II)inamide have been deposited to the Protein Data Bank, Research Collaboratory for Structural Bioinformatics, Rutgers University, New Brunswick, NJ (http://www.rcsb.org) under the PDB accession numbers 3CI1, 3CI3 and 3CI4, respectively.

[▽] Department of Biochemistry.

[§] Department of Bacteriology.

[||] Department of Chemistry.

[1] Abbreviations: ACA, ATP:co(I)rrinoid adenosyltransferase; *Lr*PduO, *Lactobacillus reuteri* PduO; Cbl, cobalamin; cbi, cobinamide; AdoCbl, adenosylcobalamin; HOCbl, hydroxycobalamin; $(CN)_2$Cbi, dicyanocobinamide; FMN, flavin mononucleotide; MES, morpholinoethanesulfonic acid; NADH, reduced nicotinamide adenine dinucleotide; Fre, flavin mononucleotide reductase; HEPES, 4-(2-hydroxyethyl)-1-piperazineethanesulfonic acid; DMB, dimethylbenzimidazole; MCD, magnetic circular dichroism; SHE, standard hydrogen electrode; CNCb1, cyanocobalamin.

10.1021/bi800132d CCC: $40.75
Published on Web 05/02/2008

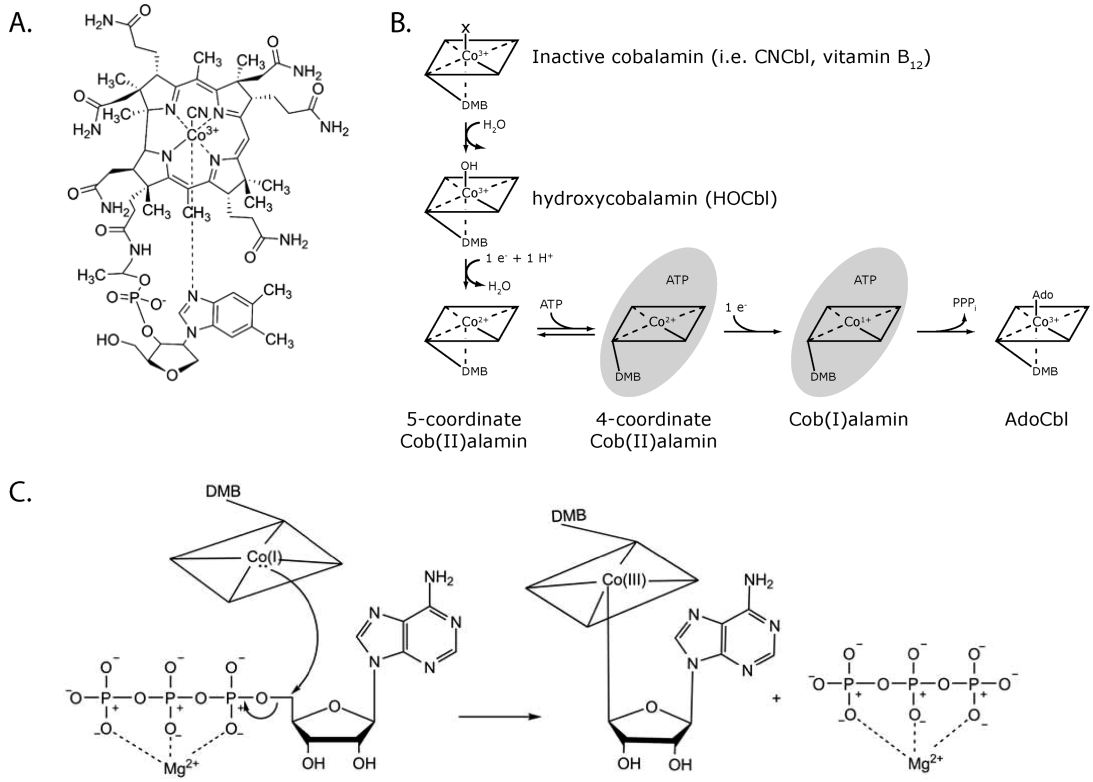

FIGURE 1: PduO-type ACA-mediated biosynthesis of coenzyme B_{12}. (A) Structural formula of vitamin B_{12} (CNCbl). (B) Proposed route for the biosynthesis of coenzyme B_{12} from vitamin B_{12}. Assimilated cob(III)alamin is reduced to cob(II)alamin in the cellular reducing environment. Cob(II)alamin is bound by ACA (gray oval), generating a four-coordinate, base-off intermediate in the presence of ATP. This facilitates a final electron transfer to generate a base-off, four-coordinate cob(I)alamin in the ACA active site. The resulting cob(I)alamin supernucleophile reacts with ATP to generate coenzyme B_{12} (AdoCbl). (C) Mechanism of cobalamin adenosylation by ACA. The reduced cob(I)alamin supernucleophile attacks the 5′-carbon of ATP to generate coenzyme B_{12} (AdoCbl) and tripolyphosphate (PPP_i).

of ATP in the ACA active site, generating AdoCbl and tripolyphosphate [PPP_i (Figure 1C)] (*14, 15*). Thus, ACA enzymes are charged with two distinct tasks. (1) They must facilitate electron transfer to cob(II)alamin by generating a four-coordinate intermediate species, and (2) they must lower the activation energy barrier for the subsequent nucleophilic attack by orienting the substrates for catalysis and stabilizing the transition state (*16*). A description of how the enzyme accomplishes either of these tasks at the molecular level remains incomplete. The structures of AdoCbl-dependent enzymes have, in some cases, shown the lower axial ligand of Cbl replaced with a histidine residue to form a His-on/base-off, five-coordinate cobalamin (*17, 18*). However, the proposed four-coordinate conformation of cob(II)alamin in ACA has not been observed in the crystal structure of any B_{12} binding protein.

Three structurally distinct types of ACA were originally identified in *Salmonella enterica*: CobA, EutT, and PduO (*15, 19, 20*). CobA is the housekeeping enzyme in *Salmonella*, while EutT and PduO play specialized roles in ethanolamine and propanediol utilization pathways, respectively. Despite its specialized role in *Salmonella*, PduO is the most widely distributed ACA enzyme, with homologues identified in species of archaea and bacteria, and eukaryotes ranging from algae to humans (*21–23*). In humans, a single PduO-type ACA enzyme is used for the generation of AdoCbl from vitamin B_{12}. Recently, X-ray crystal structures of PduO-type ACAs from *Homo sapiens* (*24*) and *Lactobacillus reuteri* (*25*) have been reported with ATP bound in the active site, revealing a unique ATP binding motif near the subunit interface. These structures revealed the bacterial and human enzymes to be very similar. While recent structural studies have attempted to determine the binding location of Cbl at the active site (*24–26*), this substrate has not yet been observed bound to any PduO-type enzyme. Since ACA function is dependent on cob(II)alamin binding and four-coordinate formation, a description of the molecular interactions with Cbl is required to improve our understanding of enzyme function and to further characterize dysfunctions that result in human disease.

We have determined the X-ray crystal structures of a PduO-type ACA from *L. reuteri* (*Lr*PduO) complexed with a four-coordinate cob(II)alamin intermediate and with the product, AdoCbl, to high resolution. The structures provide insights into the molecular basis of four-coordinate cob(II)alamin stabilization and permit the assembly of a complete description of the reaction steps in the ACA-catalyzed reaction.

EXPERIMENTAL PROCEDURES

Adenosyltransferase Assay. The *Lr*PduO protein was produced and purified as previously described (*16, 25*). Corrinoid adenosylation assays were performed under anoxic conditions at 25 °C. Stock solutions (typical volumes of 20−300 μL) were sparged with O_2-free N_2 for 2−3 min and incubated in an anoxic chamber for 1−2 h to ensure removal of O_2 from the solutions. To assay adenosylation activity under initial velocity conditions, a 2 mL reaction mixture contained the following: ATP (1 mM), $MgCl_2$ (1.5 mM),

HOCbl (0.5 mM), FMN (2 mM), NADH (20 mM), NAD(P)H:flavin oxidoreductase [Fre (*6*); 500 μg/mL], morpholinoethanesulfonic acid (MES, 100 mM, pH 6.0), and KCl (100 mM). This solution was incubated for 2 h prior to initiation of the reaction to allow complete reduction of HOCbl to cob(II)alamin. The adenosylation reaction was initiated by the addition of the *Lr*PduO protein to a final concentration of 100 μg/mL.

Adenosylation activity was also measured under reaction conditions closely approximating those in the crystallization drops. For this assay, a 1.5 mL reaction mixture contained the following: ATP (1 mM), $MgCl_2$ (1.5 mM), HOCbl (1 mM), FMN (1 mM), NADH (10 mM), Fre (50 μg/mL), MES (100 mM, pH 6.0), and KCl (100 mM). The reaction mixture was incubated for 2 h, and the reaction was initiated by the addition of the *Lr*PduO protein to a final concentration of 1 mg/mL.

All reactions were performed in an anoxic chamber (Coy Laboratory Products, Grass Lake, MI). At fixed time intervals, a 100 μL sample was removed from the reaction, diluted 1:10 with anoxic buffer containing 4-(2-hydroxyethyl)-1-piperazineethanesulfonic acid (HEPES, 100 mM, pH 8) and NaCl (500 mM), sealed in a 1 cm path length anoxic cuvette, and removed from the anoxic chamber. AdoCbl was quantified by measuring the difference in absorbance at 525 nm, before and after a 10 min photolysis of the reaction product, AdoCbl ($\Delta\epsilon_{525} = 4.8\ cm^{-1}\ mM^{-1}$) (*27*).

Spectroscopic Measurements. The sample prepared for low-temperature electronic absorption and magnetic circular dichroism (MCD) experiments was injected anoxically into a preassembled MCD cell and frozen in liquid nitrogen. All spectra were collected on a Jasco J-715 spectropolarimeter in conjunction with an Oxford Instruments SM-4000 8T magnetocryostat. To remove the contribution from the natural CD and glass strain to each MCD spectrum, the difference was taken between spectra obtained with the field aligned parallel and antiparallel to the light propagation axis. The room-temperature absorption spectrum of a single crystal was obtained using a Varian Cary 5e spectrophotometer. The crystal was embedded in epoxy resin to protect it from air oxidation, and a small piece of epoxy was placed in the reference beam to reduce contributions from the epoxy to the absorption spectrum.

Crystallization and Data Collection. The *LrPduO* protein was produced and purified as previously described (*25*). All crystals of the tag-cleaved *Lr*PduO protein were grown using the vapor diffusion method in an anoxic chamber at 25 °C. Crystals of the precatalytic Cbl complex [*Lr*PduO−ATP−cob(II)alamin] were grown by mixing 4 μL of protein solution [18 mg/mL; Fre (33 μg/mL), NADH (20 mM), FMN (2 mM), HOCbl (2 mM), ATP (3 mM), and $MgCl_2$ (3 mM)] with 4 μL of reservoir solution [polyethylene glycol 8000 (13%, w/v), KCl (200 mM), and MES (100 mM, pH 6)]. Several large, brown-colored, cubic crystals (~200 μm^3) appeared spontaneously after 18 h and were grown for an additional 4 days. The crystals were then transferred to an anoxic synthetic mother liquor solution [glycerol (2%, v/v), polyethylene glycol 8000 (10%, w/v), MES (100 mM, pH 6), KCl (200 mM), Fre (35 μg/mL), NADH (20 mM), FMN (2 mM), HOCbl (2 mM), ATP (2 mM), and $MgCl_2$ (2 mM)] and, in an anoxic chamber, incrementally transferred in five steps to an anoxic cryoprotectant solution [glycerol (20%, v/v), polyethylene glycol 8000 (12%, w/v), MES (100 mM, pH 6), KCl (300 mM), Fre (35 μg/mL), NADH (20 mM), FMN (2 mM), HOCbl (2 mM), ATP (2 mM), and $MgCl_2$ (2 mM)]. The crystals were briefly exposed to oxygen (≤5 s) while they were flash-frozen in liquid nitrogen.

Crystals of the reacted complex (*Lr*PduO−PPP_i−AdoCbl) were grown by mixing 2 μL of protein solution [22 mg/mL; Fre (30 μg/mL), NADH (20 mM), FMN (2 mM), HOCbl (2 mM), ATP (3 mM), and $MgCl_2$ (3 mM)] with 2 μL of reservoir solution [polyethylene glycol 8000 (10%, w/v) and MES (100 mM, pH 6)]. A single large, brown-colored, cubic crystal (~200 μm^3) appeared spontaneously after 2 days. After a 65 day incubation, this crystal was transferred to an anoxic synthetic mother liquor solution [glycerol (2%, v/v), polyethylene glycol 8000 (10%, w/v), MES (100 mM, pH 6), NaCl (200 mM), Fre (50 μg/mL), NADH (20 mM), FMN (2 mM), and HOCbl (2 mM)] and, in an anoxic chamber, incrementally transferred in five steps to an anoxic cryoprotectant solution [glycerol (20%, v/v), polyethylene glycol 8000 (12%, w/v), MES (100 mM, pH 6), NaCl (300 mM), Fre (50 μg/mL), NADH (20 mM), FMN (2 mM), HOCbl (2 mM), ATP (2 mM), and $MgCl_2$ (2 mM)]. The crystals were briefly exposed to oxygen (≤5 s) prior to being flash-frozen in a nitrogen stream at 100 K (Oxford Cryosystems, Oxford, U.K.).

Crystals of the precatalytic cobinamide complex [*Lr*PduO−ATP−cob(II)inamide] were grown by mixing 4 μL of protein solution [18 mg/mL; Fre (33 μg/mL), NADH (20 mM), FMN (2 mM), $(CN)_2$Cbi (2 mM), ATP (2 mM), and $MgCl_2$ (2 mM)] with 4 μL of reservoir solution [polyethylene glycol 8000 (13%, w/v), KCl (200 mM), and MES (100 mM, pH 6)]. A few large, orange-colored, cubic crystals (~150 μm^3) appeared spontaneously after 48 h and were grown for an additional 5 days. The crystals were then transferred to an anoxic synthetic mother liquor solution [glycerol (2%, v/v), polyethylene glycol 8000 (10%, w/v), MES (100 mM, pH 6), KCl (200 mM), Fre (35 μg/mL), NADH (20 mM), FMN (2 mM), $(CN)_2$Cbi (2 mM), ATP (2 mM), and $MgCl_2$ (2 mM)] and, in an anoxic chamber, incrementally transferred in five steps to an anoxic cryoprotectant solution [glycerol (20%, v/v), polyethylene glycol 8000 (12%, w/v), MES (100 mM, pH 6), KCl (300 mM), Fre (50 μg/mL), NADH (20 mM), FMN (2 mM), HOCbl (2 mM), ATP (2 mM), and $MgCl_2$ (2 mM)]. The crystals were briefly exposed to oxygen (≤5 s) while they were flash-frozen in liquid nitrogen.

All crystals belong to space group *R*3 with one subunit in the asymmetric unit. Data sets for the crystals of the precatalytic complexes [*Lr*PduO−ATP−cob(II)inamide and *Lr*PduO−ATP−cob(II)alamin] were collected at 100 K with a Bruker AXS Platinum 135 CCD detector controlled with the Proteum software suite [Bruker (2004) *PROTEUM*, Bruker AXS Inc., Madison, WI]. The X-ray source was Cu Kα radiation from a Rigaku RU200 X-ray generator equipped with Montel optics and operated at 50 kV and 90 mA. These data were processed with SAINT (version V7.06A, Bruker AXS Inc.) and internally scaled with SADABS (version 2005/1, Bruker AXS Inc.). A data set for the crystal of the reacted complex (*Lr*PduO−PPP_i−AdoCbl) was collected at the Advanced Photon Source in Argonne, IL, on beamline 19ID. Diffraction data were integrated and scaled with *HKL2000* (*28*). Data collection statistics are summarized in Table 1.

Table 1: Data Collection and Refinement Statistics

	*Lr*PduO−PPP_i−AdoCbl	*Lr*PduO−ATP−Cbl(II)	*Lr*PduO−ATP−Cbi(II)
space group	*R*3	*R*3	*R*3
cell dimensions			
a, *b*, *c* (Å)	68.0, 68.0, 110.9	67.8, 67.8, 111.2	67.8, 67.8, 111.3
α, *β*, *γ* (deg)	90, 90, 120	90, 90, 120	90, 90, 120
resolution range (Å)	30.0−1.11 (1.15−1.11)[a]	30.0−1.90 (1.95−1.90)[a]	30.0−2.00 (2.10−2.05)[a]
redundancy	4.9 (2.3)[a]	3.5 (2.2)[a]	2.5 (1.5)[a]
completeness (%)	98.9 (89.0)[a]	97.4 (98.1)[a]	98.2 (99.9)[a]
no. of unique reflections	74669	16892	13603
R_{merge} (%)	3.9 (9.6)[a]	9.3 (28.2)[a]	10.9 (26.0)[a]
average I/σ	35.3 (9.8)[a]	8.2 (2.4)[a]	5.7 (1.7)[a]
R_{cryst}	0.161 (0.205)[a]	0.157 (0.175)[a]	0.172 (0.198)[a]
R_{free}	0.180 (0.241)[a]	0.204 (0.234)[a]	0.216 (0.230)[a]
no. of protein atoms	1564	1500	1483
no. of water molecules	172	149	86
Wilson *B* value (Å^2)	13.9	19.4	20.6
average *B* factor (Å^2)			
protein	12.2	8.3	9.5
ligands	13.9	16.9	17.9
solvent	24.7	20.3	19.1
Ramachandran (%)			
most favored	97.6	98.2	97.0
additionally allowed	1.8	1.8	3.0
generously allowed	0.6	0	0
disallowed	0	0	0
root-mean-square deviation			
bond lengths (Å)	0.020	0.014	0.016
bond angles (deg)	2.39	2.05	2.07

[a] Values in parentheses are for the highest-resolution bin.

Structure Determination and Refinement. The structures were determined by molecular replacement with MOLREP (*29*) starting from the model of the wild-type *Lr*PduO protein complexed with ATP (PDB entry 2NT8). The structure of the reacted complex (*Lr*PduO−PPP_i−AdoCbl) was subjected to final refinement using loose geometric restraints (WEIGht MATRix 5), and the structures of the unreacted complexes [*Lr*PduO−ATP−cob(II)inamide and *Lr*PduO−ATP−cob(II)-alamin] were subjected to final refinement using medium geometric restraints (WEIGht MATRix 0.3), with REFMAC (*30*). Heteroatoms, water molecules, and multiple conformations were built using COOT (*31*). The final models for the *Lr*PduO−ATP−cob(II)alamin, *Lr*PduO−ATP−cob(II)-inamide, and *Lr*PduO−PPP_i−AdoCbl complexes were refined to 1.9, 2.1, and 1.1 Å, respectively. In all cases, the models include residues 1−188, comprising the complete polypeptide chain. Ramachandran plots for all models show that greater than 96% of residues are in the most favored region with no residues falling in the disallowed region. Refinement statistics are listed in Table 1.

RESULTS

Spectroscopic Characterization of Crystal Mother Liquor Components. The *Lr*PduO protein was crystallized under anoxic conditions in the presence of an accompanying enzyme system designed to reduce cob(III)alamin to cob(II)alamin. In this flavin-dependent reducing system, an NAD(P)H:flavin oxidoreductase (Fre; EC 1.6.8.1) reduces FMN to $FMNH_2$ and the reduced flavin rapidly reduces HOCbl to cob(II)alamin (*6*). The components of this system have been shown not to produce detectable levels of AdoCbl in the presence of ATP-bound CobA from *S. enterica* (*6*). Absorption spectra of the mother liquors used for crystallization, both in the presence and in the absence of the *Lr*PduO protein, exhibit a prominent feature in the visible spectral region (the so-called α-band) at 474 nm (Figure 2A, red and blue traces). This α-band position is characteristic of cob(II)alamin (dashed yellow line), demonstrating that HOCbl was stoichiometrically reduced to cob(II)alamin under the crystallization conditions. Importantly, the spectra of the mother liquors showed no evidence of cob(I)alamin.

Magnetic circular dichroism (MCD) spectroscopy offers a sensitive probe of the electronic structures of co(II)rrinoids, producing a characteristic spectrum for four-coordinate cob(II)alamin (*8–10*). The low-temperature MCD spectrum of a frozen glass of the crystal mother liquor revealed a weak but highly characteristic spectrum of four-coordinate cob(II)-alamin in the presence of *Lr*PduO (Figure 2B). The weak MCD spectrum resulted from the reduced molar ratio of *Lr*PduO to cobalamin in the crystallization drops. A much stronger MCD signal has been recorded for *Lr*PduO when its concentration is in excess over cobalamin (K. Park, P. Mera, J. C. Escalante-Semerena, and T. C. Brunold, submitted manuscript). Nevertheless, the distinct feature at 12430 cm^{-1} (804.5 nm) in the presence of the *Lr*PduO protein unambiguously indicated the presence of four-coordinate cob(II)alamin. The temperature dependence of the MCD spectrum confirmed that this peak is not a result of contamination or noise and demonstrated the feature to be specific to four-coordinate cob(II)alamin.

Unexpectedly, the absorption spectrum of the crystallization mother liquor also showed a contribution from the reaction product, AdoCbl (Figure 2A, red trace). In the 4.5 K absorption spectrum of a frozen glass of the mother liquor containing *Lr*PduO, the contribution from AdoCbl is evident from two shoulders at 17920 cm^{-1} (558 nm) and 18870 cm^{-1} (530 nm), corresponding to the α- and *β*-bands of AdoCbl, respectively. These features are not present in the mother liquor prepared in the absence of *Lr*PduO (Figure 2A, blue trace). To explore the origin of this unexpected result, single-

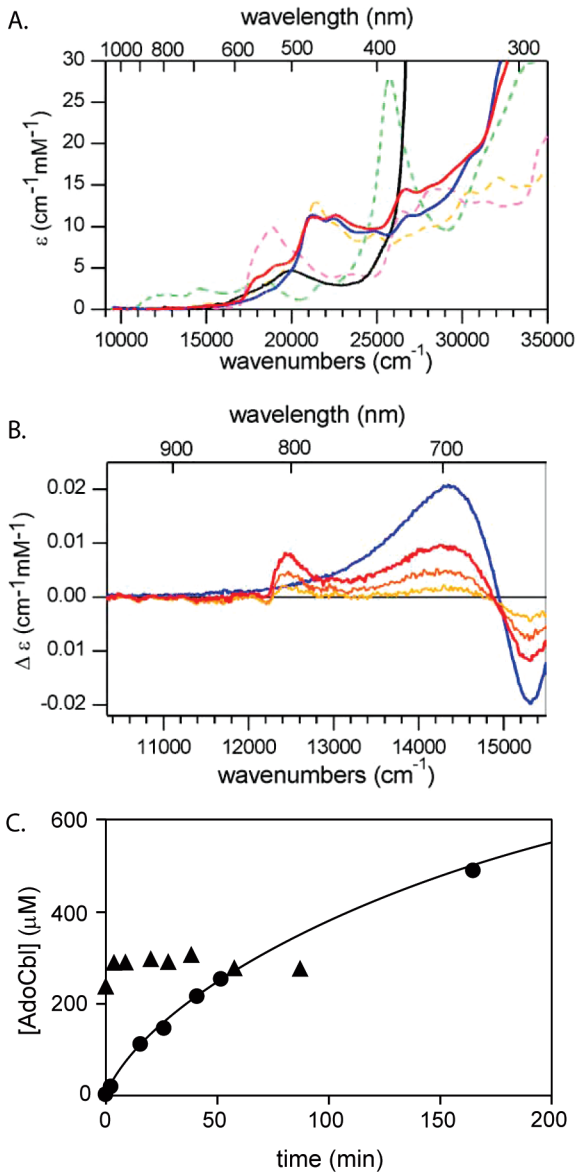

FIGURE 2: Spectroscopic and kinetic analysis of crystals and crystal mother liquor solutions. (A) Electronic absorption spectra of the crystallization mother liquor containing *Lr*PduO (solid red), the crystallization mother liquor lacking *Lr*PduO (solid blue), cob(I-I)alamin in the presence of *Lr*PduO and MgATP (dashed yellow) (K. Park, P. Mera, J. C. Escalante-Semerena, and T. C. Brunold, submitted manuscript), AdoCbl (dashed pink) (*49*), cob(I)alamin (dashed green) (*39*), and a single crystal electronic absorption spectrum (solid black). All spectra were collected at 4.5 K, except for those of cob(I)alamin (250 K) and the single crystal (room temperature). (B) MCD spectra (7 T) of the mother liquor at 4.5 (red), 10 (orange), and 25 K (yellow) and of the mother liquor in the absence of *Lr*PduO at 4.5 K (blue). All solution samples contained 60% (v/v) glycerol to ensure glass formation upon freezing. Only the low-energy region is shown. The large fraction of unbound, five-coordinate cob(II)alamin in the crystallization mother liquor prevented a conclusive interpretation of the higher-energy region. (C) AdoCbl synthesis by *Lr*PduO under crystallization conditions (▲) and under optimized initial velocity conditions (●). The assays were performed as described in Experimental Procedures.

crystal absorption spectra were collected. A representative single-crystal absorption spectrum from a crystal grown for 21 days in the same mother liquor is overlaid in Figure 2A (black trace). Most importantly, there is no spectroscopic evidence for any cob(I)alamin in the crystal. The slight shoulder at ~400 nm could not be reproduced between individual spectra and is attributed to the absorption from the epoxy resin and not from a trace amount of cob(I)alamin. Furthermore, the single-crystal absorption spectrum shows none of the lower-energy features (>600 nm) that are typical of cob(I)alamin (black trace vs dashed green trace in Figure 2A). CD spectroscopy further demonstrates the absence of any cob(I)alamin features in the crystallization mother liquors (Figure S1 of the Supporting Information). The α-band in this single-crystal absorption spectrum is centered at ~500 nm. The band is blue-shifted relative to AdoCbl and red-shifted relative to cob(II)alamin, consistent with a mixed contribution from six-coordinate AdoCbl, five-coordinate AdoCbl, and cob(II)alamin. The X-ray data collected from a similar crystal revealed electron density that corresponded to a mixture of AdoCbl and cob(II)alamin (vide infra). The steep increase in absorbance at wavelengths shorter than 380 nm resulted from the sample being mounted in epoxy resin and precluded further interpretation of the spectrum.

The 4.5 K absorption spectra of crystal mother liquors indicated that, under the conditions used for crystallization, AdoCbl is produced in the presence of the *Lr*PduO protein. To confirm that AdoCbl was being produced by *Lr*PduO in the crystallization drops, the rate of adenosylation was measured in the presence of all components of the crystal mother liquor, with the exception of polyethylene glycol 8000. The specific activity was determined to be 0.5 nmol min^{-1} mg^{-1} in the presence of ATP (1 mM), $MgCl_2$ (1.5 mM), NADH (20 mM), FMN (2 mM), HOCbl (0.5 mM), KCl (100 mM), and Fre (0.5 mg/mL) (Figure 2C, ●). Conversely, no AdoCbl was produced in the absence of the *Lr*PduO protein (data not shown). Compared to the reaction conditions described above, the crystals grew under conditions that included a 20-fold lower concentration of Fre protein, a 2-fold lower concentration of both FMN and NADH, and a 100-fold higher concentration of *Lr*PduO protein. Under these conditions, AdoCbl was generated in a rapid burst to ~300 μM (Figure 2C, ▲) and the reduced flavin pool became rapidly oxidized [as observed by an increase in the absorption peak at 450 nm corresponding to oxidized FMN (data not shown)]. At this concentration, the Fre protein did not maintain a recycled pool of $FMNH_2$, and the resulting rate of AdoCbl formation was very slow following the initial burst. Consistent with these kinetic results, spectra of crystallization solutions taken after ~72 h were calculated to contain ~20% AdoCbl. Collectively, these spectroscopic and kinetic analyses reveal that crystals were grown from a heterogeneous mother liquor containing both cob(II)alamin and AdoCbl. The crystals grew spontaneously to their maximum size within 24−48 h. During this period, the crystallization liquor was predominantly composed of cob(II)alamin and ATP but also contained 20−30% AdoCbl.

Corrinoid Binding Site of LrPduO. X-ray diffraction data were collected on a crystal grown anoxically for 5 days in the presence of MgATP, HOCbl, and the flavin reducing system. The structure was determined by molecular replacement, using initial phases from the crystal structure of *Lr*PduO complexed with MgATP (PDB entry 2NT8) (*25*). The final structure was refined to 1.9 Å resolution, with an R_{cryst} of 15.7 and an R_{free} of 20.4 (Table 1). The structure revealed that *Lr*PduO included both MgATP and Cbl bound

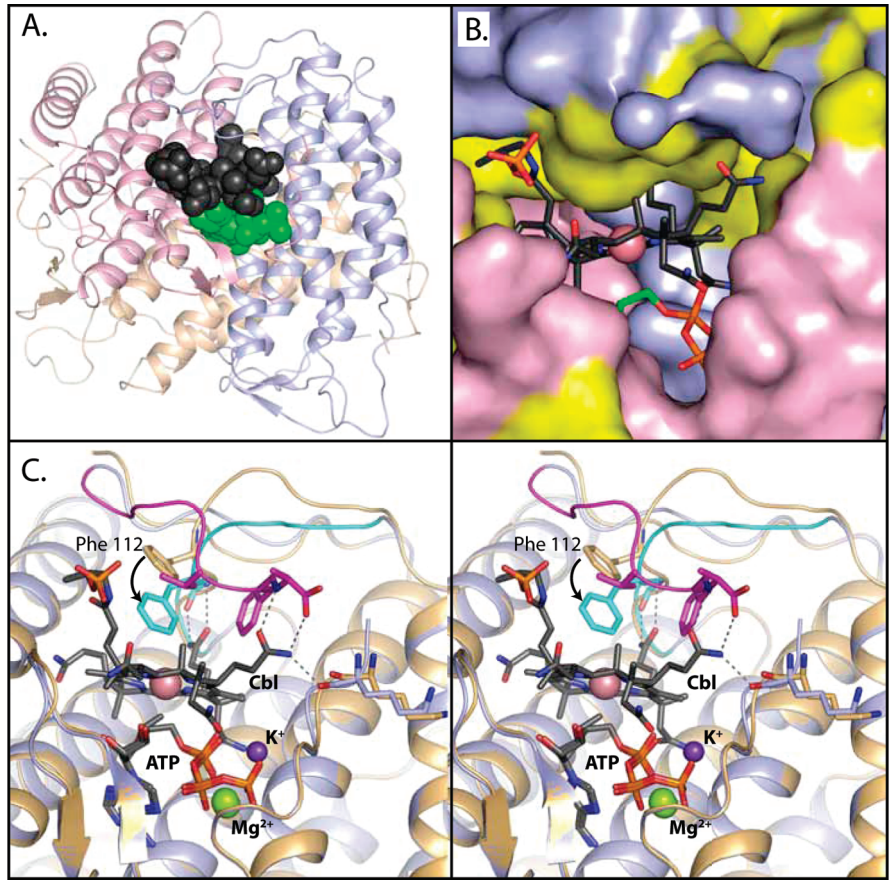

FIGURE 3: Structural overview of the *Lr*PduO active site. (A) Ribbon representation of the *Lr*PduO trimer with the individual subunits colored blue, pink, and brown. The substrates, MgATP (green spheres) and cob(II)alamin (black spheres), are denoted using a space-filling representation. Both substrates are bound in the active site, at the interface between adjacent subunits. The DMB ligand of cob(II)alamin lies outside of the active site, and the corresponding density is disordered beyond the bridging phosphate atoms. The substrates bound at the two other active sites of the trimer have been omitted for clarity. (B) Surface representation of the *Lr*PduO active site with bound cob(II)alamin (black carbon atoms) and MgATP (green carbon atoms). The *Lr*PduO subunits are colored as described above. Hydrophobic residues are colored yellow. The active site closes tightly around the cob(II)alamin substrate and completely buries MgATP in a deep cavity. A significant hydrophobic patch is centered directly above the cobalt of cob(II)alamin. (C) Stereoview of the *Lr*PduO active site with both substrates bound (blue) with the *Lr*PduO active site with only MgATP bound (brown). The position of MgATP is identical between the two structures. The binding of cob(II)alamin induces two small structural changes in the protein: (1) the C-terminus (magenta) becomes fully ordered, and (2) the loop connecting helices 3 and 4 (cyan) clamps down above the cob(II)alamin substrate, positioning Phe112 <4 Å from the cobalt of cob(II)alamin.

in the active site. *Lr*PduO is a trimer consisting of three independent five-helix bundles, with the active sites lying at the interface between adjacent monomers (Figure 3A). All three active sites of the trimer are identical and are fully occupied by both substrates. The Cbl substrate is bound in a cleft at the subunit interface, immediately above MgATP (Figure 3A). Most notably, the lower axial dimethylbenzimidazole (DMB) ligand of Cbl is pushed out of the active site and no longer coordinates to the cobalt atom. The vacant lower axial coordination site is not occupied by a water molecule or by a functional group from the protein. Rather, the protein environment in this region consists of several bulky, hydrophobic residues positioned in the proximity of the cob(II)alamin substrate (Figure 3B). These residues crowd out the lower DMB ligand without providing a replacement or allowing the binding of an exogenous ligand. The density for the DMB ligand is disordered beyond the bridging phosphate, precluding a precise definition of its position in this structure and suggesting that the DMB arm remains unbound and solvent-exposed.

Combined with the spectroscopic results presented above, the absence in the structure of both a lower and upper axial ligand conclusively demonstrates the presence of a four-coordinate cob(II)alamin species in the active site of the *Lr*PduO enzyme.

The structure of the *Lr*PduO enzyme complexed with MgATP and cob(II)alamin deviates very little from the *Lr*PduO structure complexed with MgATP alone (rmsd = 0.26 Å for the α-carbon backbone with PDB entry 2NT8). Notably, the position and arrangement of ATP are unchanged in the presence of bound cob(II)alamin. Two changes in conformation accompany the binding of cob(II)alamin and provide a mechanism for formation of the four-coordinate cob(II)alamin intermediate (Figure 3C). Whereas the immediate C-terminus of the enzyme has been disordered in all but one of the reported structures of PduO [ST1454, a PduO-type adenosyltransferase from *Sulfolobus tokodaii*, has a fully ordered C-terminus (*32*)], the six terminal residues of *Lr*PduO (Ser183−Arg188) become fully ordered in the presence of bound cob(II)alamin. Two hydrogen bonds between the terminal amino acid backbone (Arg188) and a corrinoid amide serve to clamp the C-terminus onto the bound cob(II)alamin substrate. In addition, the position of the loop connecting helices 3 and 4 is significantly altered

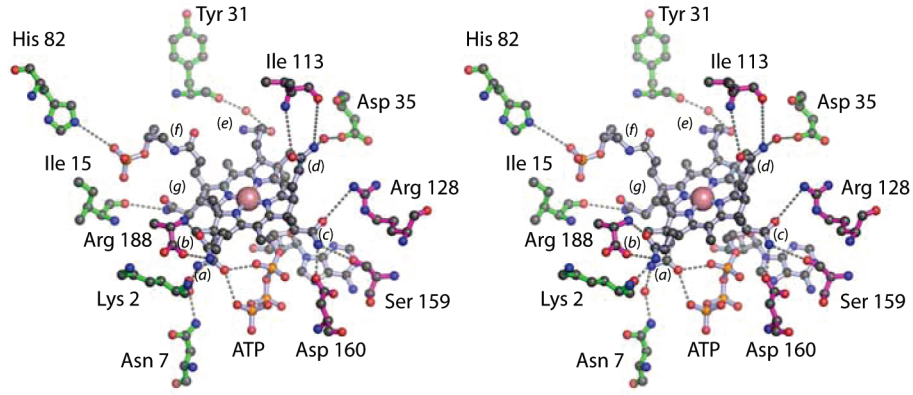

FIGURE 4: Map of interactions between *Lr*PduO and Cbl. Residues colored in green are contributed from one subunit while residues colored in magenta are contributed from an adjacent subunit. The actual positions of the side chains have been altered for illustrative-purposes. The individual amide substituents are identified by locants *a*−*f*, according to the IUPAC-IUBMB nomenclature for corrinoids (*50*). The hydrogen bond between the amide of locant *c* and Ser159 is with the main chain carbonyl and not the hydroxyl side chain. The amide substituent at locant *g* deviates slightly between the structures, and the hydrogen bond with Ile15 participates through an intervening water in the case of the *Lr*PduO−ATP−cob(II)alamin complex. The DMB ligand of cobalamin is not shown as it lies outside of the active site and the corresponding density is disordered beyond the bridging phosphate atoms.

in the presence of bound cob(II)alamin. This loop is anchored by two conserved proline residues. Pro115 is conserved across all PduO-type ACA homologues, while the second proline, Pro107, is conserved either at this position or at the preceding position in all eukaryotic and prokaryotic PduO-type ACA homologues (for detailed sequence alignments, see refs *21*, *25*, and *26*). The loop acts as a hinged lid (*33*) to fold down on the bound cob(II)alamin substrate. Two hydrogen bonds between the main chain of Ile113 and an amide substituent of cob(II)alamin lock the loop into a closed conformation. The closure of this loop significantly alters the position of Phe112 such that the carbon at the para position of the side chain's aromatic ring moves ~4 Å into the active site to occupy a position 3.8 Å from the cobalt atom of cob(II)alamin. This Phe112 residue is conserved among PduO-type ACA enzymes (*21*).

Additional hydrogen bonding interactions with the cob(II)alamin substrate involve residues from both monomer subunits and span the complete circumference of the corrin ring (Figure 4). The majority of these interactions originate from main chain amides and carbonyls. Several of these interactions are mediated through ordered water molecules. This may explain why very few of the interactions of the protein with cob(II)alamin originate from evolutionarily conserved residues. The single invariant residue is Arg128, which forms a direct contact from its side chain to a corrin ring amide.

Unlike other reported structures of PduO, the *Lr*PduO structure with bound cob(II)alamin and MgATP reveals the presence of an additional potassium ion in the active site, coordinated by the side chain of Asp160, the backbone carbonyl of Ile3, and the α- and γ-phosphates of MgATP (Figure 3C, purple sphere). The protein was crystallized in the presence of 100 mM KCl, making the functional relevance of this potassium ion unclear. While electron density has been observed at this location in other reported structures of PduO (*16, 24*), it has been assigned as a second Mg^{2+} ion in these structures. The majority of the ATP-binding determinants remain unchanged in the presence of bound cob(II)alamin, though some residues that had adopted alternate conformations in the presence of ATP alone (Arg128 and Arg132) are locked into a single conformation in the presence of cob(II)alamin. Notably, the binding of Cbl results in the movement of Tyr31 into the active site, providing an additional hydrogen bonding interaction to the 2′-OH group of ATP. This is not expected to be a common or essential feature of PduO catalysis since Tyr31 is not conserved. The equivalent position is occupied by Val in human and bovine PduO and by Leu in *S. tokadaii* PduO (*21, 32*).

Cobinamide and Cobalamin Binding Is Structurally Indistinguishable. To further investigate whether the DMB arm plays a role in positioning the corrin substrate in the active site, crystals were grown anoxically for 7 days in the presence of dicyanocobinamide [$(CN)_2$Cbi], MgATP, and the flavin reducing system. $(CN)_2$Cbi is a derivative of CNCbl that lacks the lower DMB ligand. These crystals were harvested and frozen in liquid N_2, and the X-ray diffraction data were collected. The structure revealed Cbi bound to *Lr*PduO in a manner identical to that of Cbl, suggesting that the DMB arm plays no role in positioning the substrate for catalysis (Figure S2 of the Supporting Information; rmsd = 0.07 Å for all main chain atoms). There was no electron density corresponding to a lower axial ligand for cob(II)inamide (Figure S3 of the Supporting Information). This is not surprising considering that cob(II)inamide is known to bind CN^- very poorly at neutral pH (*34*). Furthermore, sodium borohydride reduction of $(CN)_2$Cbi at pH 7 gives an MCD spectrum identical to that of reduced adenosylcobinamide and base-off cob(II)alamin (*9*), confirming that CN^- does not form an α-ligand to cob(II)inamide at neutral pH.

The finding that cob(II)alamin and cob(II)inamide are bound by *Lr*PduO in identical positions and orientations is consistent with the finding that *Lr*PduO can adenosylate Cbi with kinetic constants very similar to those for Cbl (K. Park, P. Mera, J. C. Escalante-Semerena, and T. C. Brunold, submitted manuscript). As with Cbl, Cbi is subjected to substrate inhibition at subsaturating concentrations of ATP (*16*), further supporting an identical mode of binding for the two corrinoid substrates.

AdoCbl and Tripolyphosphate Products in the LrPduO Active Site. Attempts to grow crystals in the presence of the products AdoCbl and PPP_i or in the presence of 5′-deoxyadenosine, cob(II)alamin, and PPP_i were unsuccessful.

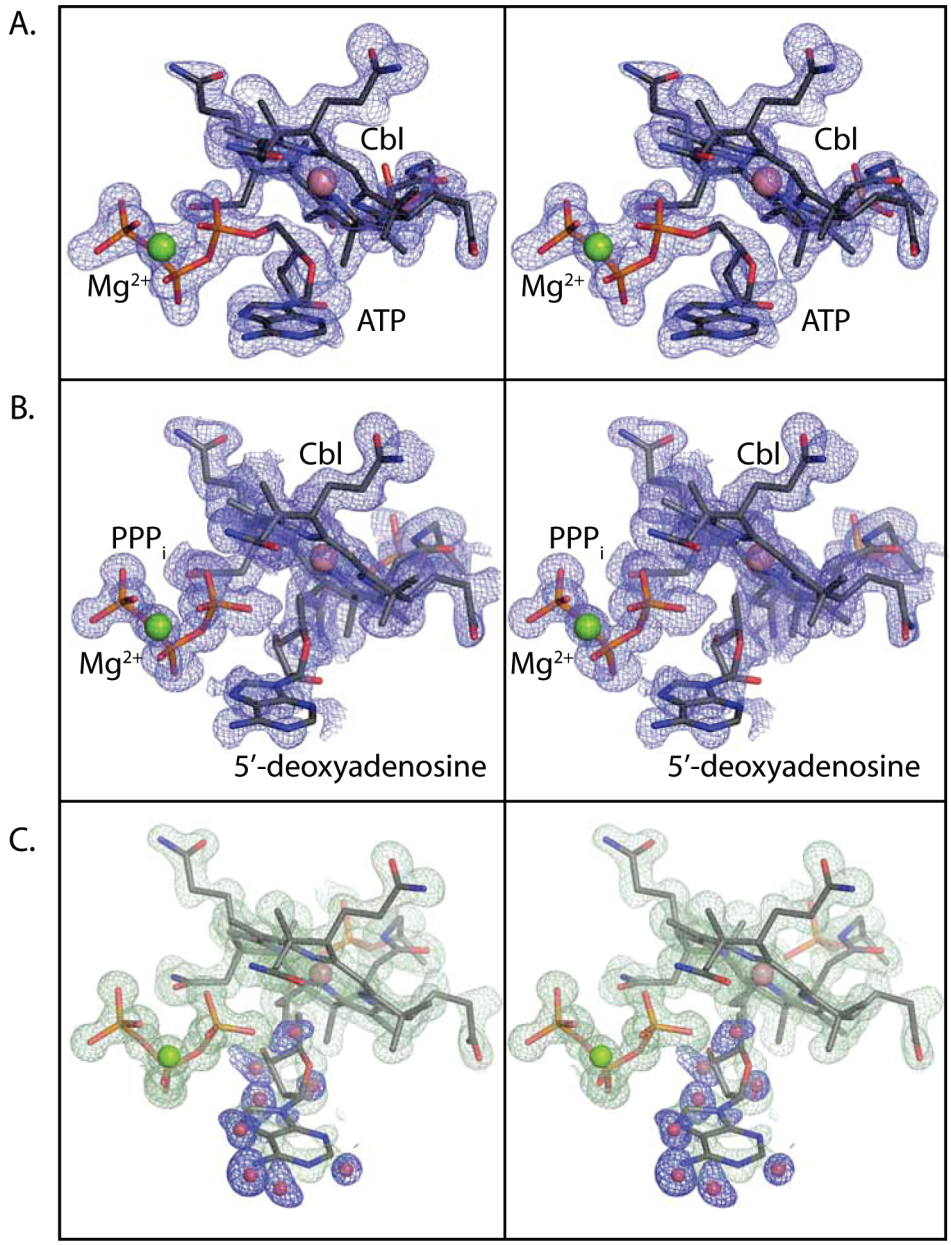

FIGURE 5: Stereoview of substrate electron densities. (A) $F_o - F_c$ electron density omit map contoured at 3σ for a 4-day-old crystal of the *Lr*PduO−ATP−cob(II)alamin complex, showing the modeled positions for MgATP and cob(II)alamin. (B) $F_o - F_c$ electron density omit map contoured at 2σ for a 65-day-old crystal showing the modeled positions for $MgPPP_i$ and AdoCbl. (C) $2F_o - F_c$ (green mesh) and $F_o - F_c$ (blue mesh) electron density omit maps contoured at 0.8σ and 2σ, respectively, after modeling the electron density for the 65-day-old crystal with cobalamin (occupancy = 1.0), $MgPPP_i$ (occupancy = 0.9), and 5′-deoxyadenosine (occupancy = 0.4). The remaining difference density can be modeled with partially occupied water molecules (red spheres; occupancy = 0.5).

A crystal incubated for 65 days in the crystallization liquor containing reduced cobalamin and MgATP diffracted to better than 1.1 Å resolution with synchrotron radiation (Table 1) but had poorly ordered density corresponding to the adenosine moiety of ATP. Rather, the electron density was best modeled as fully occupied PPP_i with partially occupied adenosine and partially occupied water molecules (Figure 5). The prolonged incubation allowed sufficient time for the slow conversion of substrates to the products AdoCbl and PPP_i. Most notably, the 5′-carbon of the adenosine ring was shifted from its previous position in the cob(II)alamin−ATP structure and was positioned at a distance and angle consistent with a covalent carbon−cobalt bond with Cbl. The electron density was incomplete between the carbon and the cobalt; however, this bond is known to be labile under X-rays (*35*), and the observed density was similar to what has been reported for AdoCbl in 5,6-lysine aminomutase (*36*). Thus, the electron density was modeled as partially occupied five-coordinate AdoCbl in the enzyme active site. Aside from the shift in the position of the 5′-carbon, the remaining conformation of *Lr*PduO was unchanged (rmsd = 0.09). Thus, no significant structural changes accompany the conversion of substrates into products in *Lr*PduO.

DISCUSSION

To catalyze the transfer of the 5′-deoxyadenosyl group from ATP to Cbl, ACA enzymes must both facilitate the reduction of cob(II)alamin to cob(I)alamin and lower the

reaction energy barrier for catalysis through favorable substrate orientation and transition state stabilization (*16*). Spectroscopic studies have demonstrated that ACAs form a rare, four-coordinate cob(II)alamin species exclusively in the presence of ATP (*8, 10, 37*). This unusual coordination environment facilitates the reduction of cob(II)alamin to cob(I)alamin by raising the midpoint reduction potential into a range compatible with electron transfer proteins and cellular reductases (*5, 8*). In this way, ACA enzymes limit the formation of the highly reactive cob(I)alamin supernucleophile to the controlled environment of the enzyme active site, where C5′ of ATP is preoriented to serve as the electrophile in the reaction.

In the absence of structural information detailing the binding of Cbl in the active site, the molecular basis for four-coordinate cob(II)alamin formation and orientation in PduO-type ACA enzymes has remained unclear. Previous attempts to cocrystallize PduO enzymes with cob(III)alamin failed to yield interpretable electron density for the Cbl substrate (*24–26*). This was likely a result of the poor binding affinity of cob(III)alamin for the enzyme. To overcome this problem, the *Lr*PduO protein was crystallized under anoxic conditions in the presence of an accompanying enzyme system designed to reduce cob(III)alamin to cob(II)alamin (*6*).

Four-Coordinate Cob(II)alamin Formation in LrPduO. Crystals harvested after 5 days reveal unambiguous electron density for cob(II)alamin and ATP in the enzyme active site (Figure 5A) and offer insight into the organization of the precatalytic complex. Spectroscopic data confirm that neither cob(III)alamin nor cob(I)alamin is present in the crystallization solutions. Most strikingly, there is no observed electron density that could account for an ordered water molecule serving as an axial ligand to the cobalt atom. This offers clear, visual evidence that cob(II)alamin is bound in a base-off, four-coordinate conformation, as predicted by spectroscopic studies (*8–10*).

Unlike the base-off form of bound Cbl in the class I Cbl-dependent isomerases (*38*), in *Lr*PduO the DMB lower ligand of Cbl is removed without being replaced by an enzyme-derived histidine. Rather, the DMB portion of cob(II)alamin is pushed out of the active site by bulky, hydrophobic residues that create spatial constraints on binding Cbl in a tight, hydrophobic pocket (Figure 3B). The structure of cob(II)inamide bound in the active site is identical to that of cob(II)alamin (Figure S2 of the Supporting Information), further confirming that there are no significant binding determinants within the nucleotide loop that influence the position or orientation of the corrin ring in the active site. This is consistent with reported K_M and K_d values for PduO-type ACAs that reveal similar constants between the substrates Cbi and Cbl (*37*) (K. Park, P. Mera, J. C. Escalante-Semerena, and T. C. Brunold, submitted manuscript).

Concomitant with Cbl binding in the active site, a loop connecting helices 3 and 4 changes orientation to create several contacts with side chain amides of the corrin ring (Figure 3C). In so doing, this loop clamps down over the active site and displaces the DMB ligand into solvent. A conserved Phe residue (Phe112) is positioned at the furthest extremity of this loop and moves to within 3.8 Å of the cobalt ion. This loop exhibits many features of a hinged lid (*33*). In the absence of bound Cbl, the loop is in an "open" conformation, while in the presence of bound Cbl, the loop adopts a "closed" conformation (Figure 3C). The conformation of this loop varies precisely between two conserved Pro residues (Pro115 and Pro107). Interestingly, the structure of ST1454 (*32*), a PduO-type ACA from *S. tokadaii*, also has the hinged lid in a closed conformation and positions a Phe in a position equivalent to that of Phe112 in *Lr*PduO. ST1454 is also the only other reported PduO-type ACA with a fully ordered C-terminus. In ST1454, a polypropylene glycol molecule is bound in the Cbl binding pocket. The presence of this molecule may be sufficient to induce loop closure analogous to that induced by the corrinoid substrates in *Lr*PduO.

The coordination environment of the cob(II)alamin substrate in the closed active site explains the ability of *Lr*PduO to facilitate reduction to cob(I)alamin. Displacing the lower DMB ligand serves to destabilize cob(II)alamin in its ground state and forces it into a conformation analogous to the product, cob(I)alamin. As such, the reduction of cob(II)alamin becomes more energetically favorable (*39*). In a classic Circe effect (*40*), the favorable enthalpy associated with substrate binding pays for this ground-state destabilization. The hydrophobic environment surrounding the corrin ring further favors the reduction of positive charge that accompanies the conversion of cob(II)alamin to cob(I)alamin.

Adenosylcobalamin Synthesis and Structural Characterization. Both spectroscopic and kinetic studies confirm that, under the crystallization conditions, AdoCbl is synthesized by *Lr*PduO at a slow rate (Figure 2). This is in contrast to the results obtained in both *Salmonella* CobA and human PduO-type ACA, which revealed no detectable rate of AdoCbl formation in the absence of a cob(II)alamin/cob(I)alamin electron transfer protein or reductase (*6, 12*). For *Lr*PduO to catalyze adenosylation with the reducing system presented here, cob(I)alamin must be generated in the absence of a specific reductase. This can occur either through a direct electron transfer to cob(II)alamin or through the natural disproportionation of cob(II)alamin (*6, 41*). The unique ability of *Lr*PduO to adenosylate Cbl in this system may be related to its unusually low K_M for cob(I)alamin (*25*), allowing it to catalyze the reaction more rapidly at low concentrations. Further studies are required to distinguish between direct reduction and disproportionation and are beyond the scope of this study.

The electron density obtained from the 65-day-old crystal is best interpreted as partially occupied AdoCbl and PPP_i and partially occupied cob(II)alamin and PPP_i, with water molecules occupying the space vacated by ATP (Figure 5C). The partially occupied cob(II)alamin reveals an ordered water molecule serving as an upper ligand to yield a five-coordinate species. Ligand coordination on the upper face of cob(II)alamin is consistent with the small molecule crystal structure of heptamethylcob(II)yrinate, which shows the axial ligand preferentially coordinated to the β-face of the corrin ring (*42*). The partially occupied water-liganded cob(II)alamin in the presence of PPP_i is consistent with the recent demonstration that Cbl can bind nonproductively to *Lr*PduO, even in the absence of ATP (*16*). In this instance, a water molecule in the empty adenosine binding pocket occupies the upper axial coordination site of Co^{2+}, resulting in a five-coordinate cob(II)alamin species. Recent spectroscopic analysis of *Lr*PduO reveals ~30% base-off, water-coordinated

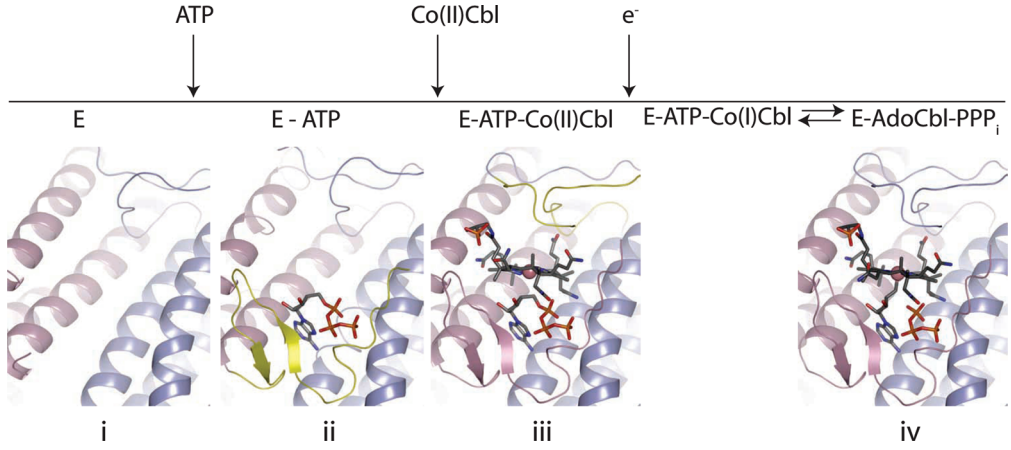

FIGURE 6: Snapshots of ACA catalysis in a PduO-type enzyme. (i) Apoenzyme with disordered N- and C-termini (from the homologous Yvqk of *Bacillus subtilis*; PDB entry 1RTY). (ii) MgATP is bound first in the enzyme active site (*16*), resulting in the ordering of the N-terminus which folds into a unique ATP binding pocket (*24, 25*) (from the structure of *Lr*PduO complexed with MgATP; PDB entry 2NT8). The ordered N-terminus is highlighted in yellow. (iii) Cob(II)alamin binds second in the enzyme active site (*16*), resulting in the ordering of the C-terminus and the closure of a hinged lid (both highlighted in yellow) to generate a four-coordinate cob(II)alamin intermediate. (iv) Following electron transfer to generate the cob(I)alamin nucleophile, AdoCbl and PPP_i are formed in the active site. The AdoCbl product is poised for direct transfer to a downstream enzyme.

cob(II)alamin in the absence of ATP (K. Park, P. Mera, J. C. Escalante-Semerena, and T. C. Brunold, submitted manuscript).

Structural Snapshots of the PduO-Catalyzed Reaction. In light of the recently proposed ordered binding mechanism for *Lr*PduO (*16*), the structural models permit the assembly of a complete set of snapshots describing the catalytic steps in coenzyme B_{12} synthesis (Figure 6). The positioning and orientation of Co^{2+} and C5′ are well suited for a subsequent S_N2 nucleophilic attack from cob(I)alamin on C5′ of ATP. Notably, Cbl is not perfectly centered above C5′. This allows the C5′−O bond to be in line for S_N2 nucleophilic attack, making an angle of 153° to Co^{2+} of cob(II)alamin. The product of the reaction, AdoCbl, is bound in a nearly identical orientation, further suggesting that the position of the substrates is unlikely to change significantly when cob(II)alamin is reduced to cob(I)alamin. AdoCbl remains in a base-off conformation, with the DMB ligand extending away from the active site. The similarity in the conformations of B_{12} between the enzymes that synthesize and utilize the coenzyme has fueled speculation that ACA enzymes also function to directly chaperone the cofactor to downstream targets (*37, 43, 44*). The observation of partially occupied AdoCbl in the PduO active site is consistent with the high binding affinity of AdoCbl for the human ACA (*37*) and further supports the possibility of a chaperone-like activity for PduO. In addition, the exclusion of the DMB arm from the enzyme active site provides an ideal binding determinant for interactions with downstream enzymes and for the efficient transfer of the coenzyme between active sites.

Insights into Enzyme Dysfunction Resulting in Methylmalonic Aciduria. Recent structural and kinetic characterizations of PduO-type ACAs have offered valuable insight into the molecular basis of enzyme dysfunction leading to methylmalonic aciduria (*16, 24–26*). This structure offers additional insight into three characterized homozygous mutations in human patients suffering from methylmalonic aciduria: R186W, S174L, and the C-terminal truncation Q234X (*45*). Mutation of Arg186 to a tryptophan in the human enzyme (R186W) is particularly common in patients suffering from methylmalonic aciduria. The structurally equivalent residue in *Lr*PduO, Arg128, was recently shown to influence ATP binding through the formation of a critical salt bridge with Asp35 (*16*). In addition to this role, this structure demonstrates that Arg128 directly interacts with the bound cob(II)alamin substrate. Disruptions in this interaction are likely to impair the binding and proper orientation of the Cbl substrate. A homozygous S174L mutation in the human ACA has been shown to result in a late clinical presentation of acidosis (*45*). In *Lr*PduO, the structurally equivalent residue, Gly116, is immediately adjacent to the conserved Pro115 that serves as a hinge of the lid that displaces the DMB ligand. Mutation of this residue to Leu may disrupt the loop structure and dynamics, disfavoring lid closure. Both Gly116 and Gly117 in *Lr*PduO adopt backbone torsion angles unique to glycine. Consequently, mutations at or near this position will strain the backbone conformation immediately adjacent to the hinged lid. Indeed, a similar mutation in tryptophan synthase immediately adjacent to a hinged lid resulted in a sizable reduction in ligand binding affinity (*46*). Several additional mutations characterized in patients suffering from methylmalonic aciduria, including G97E and S180W (*45*), are in the spatial proximity to the hinged lid and may disrupt enzyme function by interfering with loop dynamics.

Truncation of the final 16 residues in human ACA by a homozygous nonsense mutation (Q234X) has also been shown to result in an early onset of methylmalonic aciduria (*45*). The C-terminus becomes ordered upon Cbl binding and forms part of the hydrophobic pocket that excludes DMB and generates the four-coordinate intermediate. Loss of these terminal amino acids is likely to decrease the efficiency of four-coordinate cob(II)alamin formation and, thus, to disfavor the reduction of cob(II)alamin to cob(I)alamin. Detailed kinetic and spectroscopic analyses of these mutations are in progress to determine their impact on four-coordinate cob(II)alamin formation and cob(I)alamin adenosylation by *Lr*PduO.

CONCLUSION

ACA enzymes must perform several distinct tasks as they carry out the final step in coenzyme B_{12} biosynthesis. The enzyme must facilitate electron transfer, must promote catalysis, and may act to directly chaperone the reaction product to downstream enzymes. The structures of *Lr*PduO complexed with corrinoid substrates demonstrate that substrate binding promotes the ordering of a tight, hydrophobic pocket that displaces the lower DMB ligand to yield a rare, four-coordinate cob(II)alamin species. The DMB ligand remains unbound throughout the reaction, supporting recent suggestions that the base-off conformation of AdoCbl may facilitate transfer of the reaction product to coenzyme B_{12}-dependent enzymes. Spectroscopic evidence has demonstrated that cob(II)alamin stabilization is an important mechanistic feature not only among ACA enzymes (*8, 10*) but also in the Cbl-dependent enzymes methylmalonyl-CoA mutase (*47*) and methionine synthase (*48*). The strategies described here for "trapping" a partially reduced Cbl substrate in the enzyme active site may be generally amenable to crystallization of other cob(II)alamin stabilizing enzymes. Additional structural information from a range of Cbl-binding proteins will help to clarify, at a molecular level, how this aspect of catalysis is accomplished in an essential group of structurally and functionally diverse enzymes.

SUPPORTING INFORMATION AVAILABLE

CD spectra of crystallization and reference solutions further demonstrating the absence of cob(I)alamin in the crystallization solutions (Figure S1), a structural overlay of Cbi and Cbl bound to *Lr*PduO (Figure S2), and electron density for the structure of Cbi bound to *Lr*PduO (Figure S3). This material is available free of charge via the Internet at http://pubs.acs.org.

REFERENCES

1. Warren, M. J., Raux, E., Schubert, H. L., and Escalante-Semerena, J. C. (2002) The biosynthesis of adenosylcobalamin (vitamin B_{12}). *Nat. Prod. Rep. 19*, 390–412.
2. Banerjee, R., and Vlasie, M. (2002) Controlling the reactivity of radical intermediates by coenzyme B_{12}-dependent methylmalonyl-CoA mutase. *Biochem. Soc. Trans. 30*, 621–624.
3. Banerjee, R., and Chowdhury, S. (1999) Methylmalonyl-CoA mutase, in *Chemistry and Biochemistry of B12* (Banerjee, R., Ed.) pp 707−729, John Wiley & Sons, Inc., New York.
4. Rosenblatt, D. S., and Fenton, W. A. (1999) Inborn errors of cobalamin metabolism, in *Chemistry and Biochemistry of B12* (Banerjee, R., Ed.) pp 367−384, John Wiley & Sons, Inc., New York.
5. Lexa, D., and Saveant, J.-M. (1983) The electrochemistry of vitamin B_{12}. *Acc. Chem. Res. 16*, 235–243.
6. Fonseca, M. V., and Escalante-Semerena, J. C. (2000) Reduction of cob(III)alamin to cob(II)alamin in *Salmonella enterica* Serovar Typhimurium LT2. *J. Bacteriol. 182*, 4304–4309.
7. Vetter, H., Jr., and Knappe, J. (1971) Flavodoxin and ferredoxin of *Escherichia coli*. *Hoppe-Seyler's Z. Physiol. Chem. 352*, 433–446.
8. Stich, T. A., Yamanishi, M., Banerjee, R., and Brunold, T. C. (2005) Spectroscopic evidence for the formation of a four-coordinate Co(2+)cobalamin species upon binding to the human ATP:Cobalamin adenosyltransferase. *J. Am. Chem. Soc. 127*, 7660–7661.
9. Stich, T. A., Buan, N. R., and Brunold, T. C. (2004) Spectroscopic and computational studies of Co(2+)corrinoids: Spectral and electronic properties of the biologically relevant base-on and base-off forms of Co(2+)cobalamin. *J. Am. Chem. Soc. 126*, 9735–9749.
10. Stich, T. A., Buan, N. R., Escalante-Semerena, J. C., and Brunold, T. C. (2005) Spectroscopic and computational studies of the ATP:Corrinoid adenosyltransferase (CobA) from *Salmonella enterica*: Insights into the mechanism of adenosylcobalamin biosynthesis. *J. Am. Chem. Soc. 127*, 8710–8719.
11. Fonseca, M. V., and Escalante-Semerena, J. C. (2001) An in vitro reducing system for the enzymic conversion of cobalamin to adenosylcobalamin. *J. Biol. Chem. 276*, 32101–32108.
12. Leal, N. A., Olteanu, H., Banerjee, R., and Bobik, T. A. (2004) Human ATP:Cob(I)alamin adenosyltransferase and its interaction with methionine synthase reductase. *J. Biol. Chem. 279*, 47536–47542.
13. Buan, N. R., and Escalante-Semerena, J. C. (2005) Computer-assisted docking of flavodoxin with the ATP:Co(I)rrinoid adenosyltransferase (CobA) enzyme reveals residues critical for protein-protein interactions but not for catalysis. *J. Biol. Chem. 280*, 40948–40956.
14. Fonseca, M. V., Buan, N. R., Horswill, A. R., Rayment, I., and Escalante-Semerena, J. C. (2002) The ATP:co(I)rrinoid adenosyltransferase (CobA) enzyme of *Salmonella enterica* requires the 2′-OH group of ATP for function and yields inorganic triphosphate as its reaction byproduct. *J. Biol. Chem. 277*, 33127–33131.
15. Johnson, C. L., Buszko, M. L., and Bobik, T. A. (2004) Purification and initial characterization of the *Salmonella enterica* PduO ATP:Cob(I)alamin adenosyltransferase. *J. Bacteriol. 186*, 7881–7887.
16. Mera, P. E., St Maurice, M., Rayment, I., and Escalante-Semerena, J. C. (2007) Structural and Functional Analyses of the Human-Type Corrinoid Adenosyltransferase (PduO) from *Lactobacillus reuteri*. *Biochemistry 46*, 13829–13836.
17. Mancia, F., Keep, N. H., Nakagawa, A., Leadlay, P. F., McSweeney, S., Rasmussen, B., Bosecke, P., Diat, O., and Evans, P. R. (1996) How coenzyme B_{12} radicals are generated: The crystal structure of methylmalonyl-coenzyme A mutase at 2 Å resolution. *Structure 4*, 339–350.
18. Drennan, C. L., Huang, S., Drummond, J. T., Matthews, R. G., and Ludwig, M. L. (1994) How a protein binds B_{12}: A 3.0 Å X-ray structure of B_{12}-binding domains of methionine synthase. *Science 266*, 1669–1674.
19. Buan, N. R., Suh, S. J., and Escalante-Semerena, J. C. (2004) The *eutT* gene of *Salmonella enterica* encodes an oxygen-labile, metal-containing ATP:corrinoid adenosyltransferase enzyme. *J. Bacteriol. 186*, 5708–5714.
20. Suh, S., and Escalante-Semerena, J. C. (1995) Purification and initial characterization of the ATP:corrinoid adenosyltransferase encoded by the *cobA* gene of *Salmonella typhimurium*. *J. Bacteriol. 177*, 921–925.
21. Leal, N. A., Park, S. D., Kima, P. E., and Bobik, T. A. (2003) Identification of the human and bovine ATP:cob(I)alamin adenosyltransferase cDNAs based on complementation of a bacterial mutant. *J. Biol. Chem. 278*, 9227–9234.
22. Croft, M. T., Lawrence, A. D., Raux-Deery, E., Warren, M. J., and Smith, A. G. (2005) Algae acquire vitamin B_{12} through a symbiotic relationship with bacteria. *Nature 438*, 90–93.
23. Watanabe, F., Nakano, Y., Tamura, Y., and Yamanaka, H. (1991) Vitamin B_{12} metabolism in a photosynthesizing green alga *Chlamydomonas reinhardtii*. *Biochim. Biophys. Acta. 1075*, 36–41.
24. Schubert, H. L., and Hill, C. P. (2006) Structure of ATP-bound human ATP:cobalamin adenosyltransferase. *Biochemistry 45*, 15188–15196.
25. St Maurice, M., Mera, P. E., Taranto, M. P., Sesma, F., Escalante-Semerena, J. C., and Rayment, I. (2007) Structural characterization of the active site of the PduO-type ATP:Co(I)rrinoid adenosyltransferase from *Lactobacillus reuteri*. *J. Biol. Chem. 282*, 2596–2605.
26. Saridakis, V., Yakunin, A., Xu, X., Anandakumar, P., Pennycooke, M., Gu, J., Cheung, F., Lew, J. M., Sanishvili, R., Joachimiak, A., Arrowsmith, C. H., Christendat, D., and Edwards, A. M. (2004) The structural basis for methylmalonic aciduria. The crystal structure of archaeal ATP:cobalamin adenosyltransferase. *J. Biol. Chem. 279*, 23646–23653.
27. Vitols, E., Walker, G. A., and Huennekens, F. M. (1966) Enzymatic conversion of vitamin B_{12}s to a cobamide coenzyme, alphawolf-(5,6-dimethylbenzimidazolyl)deoxy-adenosylcobamide (adenosyl-B_{12}). *J. Biol. Chem. 241*, 1455–1461.
28. Otwinowski, Z., and Minor, W. (1997) Processing of X-ray diffraction data collected in oscillation mode. *Methods Enzymol. 276*, 307–326.

29. Vagin, A., and Teplyakov, A. (1997) MOLREP: An Automated Program for Molecular Replacement. *J. Appl. Crystallogr. 30*, 1022–1025.
30. Murshudov, G. N., Vagin, A. A., and Dodson, E. J. (1997) Refinement of macromolecular structures by the Maximum-Likelihood Method. *Acta Crystallogr. D53*, 240–255.
31. Emsley, P., and Cowtan, K. (2004) Coot: Model-building tools for molecular graphics. *Acta Crystallogr. D60*, 2126–2132.
32. Tanaka, Y., Sasaki, T., Kumagai, I., Yasutake, Y., Yao, M., Tanaka, I., and Tsumoto, K. (2007) Molecular properties of two proteins homologous to PduO-type ATP:cob(I)alamin adenosyltransferase from *Sulfolobus tokodaii*. *Proteins 68*, 446–457.
33. Joseph, D., Petsko, G. A., and Karplus, M. (1990) Anatomy of a conformational change: Hinged "lid" motion of the triosephosphate isomerase loop. *Science 249*, 1425–1428.
34. Bayston, J. H., Looney, F. D., Pilbrow, J. R., and Winfield, M. E. (1970) Electron paramagnetic resonance studies of cob(II)alamin and cob(II)inamides. *Biochemistry 9*, 2164–2172.
35. Champloy, F., Gruber, K., Jogl, G., and Kratky, C. (2000) XAS spectroscopy reveals X-ray-induced photoreduction of free and protein-bound B_{12} cofactors. *J. Synchrotron Radiat. 7*, 267–273.
36. Berkovitch, F., Behshad, E., Tang, K. H., Enns, E. A., Frey, P. A., and Drennan, C. L. (2004) A locking mechanism preventing radical damage in the absence of substrate, as revealed by the X-ray structure of lysine 5,6-aminomutase. *Proc. Natl. Acad. Sci. U.S.A. 101*, 15870–15875.
37. Yamanishi, M., Labunska, T., and Banerjee, R. (2005) Mirror "base-off" conformation of coenzyme B_{12} in human adenosyltransferase and its downstream target, methylmalonyl-CoA mutase. *J. Am. Chem. Soc. 127*, 526–527.
38. Banerjee, R., and Ragsdale, S. W. (2003) The many faces of vitamin B_{12}: Catalysis by cobalamin-dependent enzymes. *Annu. Rev. Biochem. 72*, 209–247.
39. Liptak, M. D., and Brunold, T. C. (2006) Spectroscopic and computational studies of Co(1+)cobalamin: Spectral and electronic properties of the "superreduced" B_{12} cofactor. *J. Am. Chem. Soc. 128*, 9144–9156.
40. Jencks, W. P. (1975) Binding energy, specificity, and enzymic catalysis: the circe effect. *Adv. Enzymol. Relat. Areas Mol. Biol. 43*, 219–410.
41. Yamada, R.-H., Schimizu, S., and Fukui, S. (1968) Disproportionation of vitamin B12r under various mild conditions. *Biochemistry 7*, 1713–1719.
42. Kräutler, B., Keller, W., Hughes, M., Caderas, C., and Kratky, C. (1987) A crystalline cobalt(II)corrinate derived from vitamin B_{12}: Preparation and X-ray crystal structure. *J. Chem. Soc., Chem. Commun.,* 1678–1680.
43. Banerjee, R. (2006) B_{12} trafficking in mammals: A case for coenzyme escort service. *ACS Chem. Biol. 1*, 149–159.
44. Yamanishi, M., Vlasie, M., and Banerjee, R. (2005) Adenosyltransferase: An enzyme and an escort for coenzyme B_{12}? *Trends Biochem. Sci. 30*, 304–308.
45. Lerner-Ellis, J. P., Gradinger, A. B., Watkins, D., Tirone, J. C., Villeneuve, A., Dobson, C. M., Montpetit, A., Lepage, P., Gravel, R. A., and Rosenblatt, D. S. (2006) Mutation and biochemical analysis of patients belonging to the cblB complementation class of vitamin B12-dependent methylmalonic aciduria. *Mol. Genet. Metab. 87*, 219–225.
46. Brzovic, P. S., Hyde, C. C., Miles, E. W., and Dunn, M. F. (1993) Characterization of the functional role of a flexible loop in the α-subunit of tryptophan synthase from *Salmonella typhimurium* by rapid-scanning, stopped-flow spectroscopy and site-directed mutagenesis. *Biochemistry 32*, 10404–10413.
47. Brooks, A. J., Vlasie, M., Banerjee, R., and Brunold, T. C. (2005) Co-C bond activation in methylmalonyl-CoA mutase by stabilization of the post-homolysis product Co(2+) cobalamin. *J. Am. Chem. Soc. 127*, 16522–16528.
48. Liptak, M. D., Fleischhacker, A. S., Matthews, R. G., and Brunold, T. C. (2007) Probing the role of the histidine 759 ligand in cobalamin-dependent methionine synthase. *Biochemistry 46*, 8024–8035.
49. Stich, T. A., Brooks, A. J., Buan, N. R., and Brunold, T. C. (2003) Spectroscopic and computational studies of Co(3+)-corrinoids: Spectral and electronic properties of the B_{12} cofactors and biologically relevant precursors. *J. Am. Chem. Soc. 125*, 5897–5914.
50. Hoffmann-Ostenhof, O., Cohn, W. E., Braunstein, A. E., Horecker, B. L., Karlson, P., Keil, B., Klyne, W., LiBbecq, C., Webb, E. C., and Whelan, W. J. (1974) The Nomenclature of Corrinoids. *Arch. Biochem. Biophys. 161*, iii–xi.

BI800132D